Article Title
Experimental monitoring of bridge frequency evolution during the passage of vehicles with different suspension properties

Authors
Daniel Cantero (1)
Patrick McGetrick (2)
Chul-Woo Kim (3)
Eugene OBrien (4)

Affiliations
(1) Department of Structural Engineering, Norwegian University of Science & Technology NTNU, Trondheim, Norway
(2) SNBE, David Keir Building, Queen's University Belfast, BT9 5AG, UK
(3) Department of Civil and Earth Resources Engineering, Kyoto University, Kyoto 615-8540, Japan
(4) School of Civil Engineering, University College Dublin, Newstead, Belfield, Dublin 4, Ireland

Manuscript version
Post-print = Final draft post-refereeing, before copy-editing by journal

DOI:
https://doi.org/10.1016/j.engstruct.2019.02.065

Reference:

Cantero, D., McGetrick, P., Kim, C.W., OBrien, E.J. (2019) Experimental monitoring of bridge frequency evolution during the passage of vehicles with different suspension properties. *Engineering Structures*, Vol. 187, pp. 209-219.

Abstract

The natural frequencies of coupled vehicle-bridge systems change with vehicle position. These changes are generally attributed to the contribution of the additional mass of the vehicle. However, other mechanical properties of the vehicle influence the evolution of the vehicle-bridge system frequencies, an aspect that has rarely been addressed. The aim of this paper is to further explore how frequencies vary during a vehicle passage and empirically show that the frequency shift depends also on the vehicle-to-bridge frequency ratio. The responses of a scaled model of a vehicle traversing a bridge are measured and analysed. The signals are processed in the time-frequency domain to assess the non-stationary and non-linear nature of the responses. The interpretation is supported with the predictions of a coupled vehicle and bridge numerical model. The results confirm different frequency shifts for vehicles with the same mass but different suspension properties. Furthermore, the direct (sensor on bridge) and indirect (sensor on vehicle) methods of extracting the bridge fundamental frequency are compared. The implications of these findings for indirect or drive-by bridge monitoring techniques are discussed.

Keywords
Vehicle-bridge interaction; bridge drive-by monitoring, structural health monitoring; non-stationary system; wavelets; dynamics.

1. Introduction

Recent decades have seen the development and implementation of structural health monitoring (SHM) approaches for the condition assessment of structures such as bridges [1-4]. Methods include vibration-based monitoring of bridge modal parameters, which usually involve direct instrumentation of the bridge with sensors, e.g. accelerometers to measure ambient or traffic-induced vibration. In recent years, alternative bridge monitoring methods have been proposed which aim to extract bridge modal parameters from the dynamic response of a vehicle passing over the bridge [5, 6]. Such methods are referred to as indirect or drive-by bridge monitoring [7]. All the sensing and data acquisition equipment is contained within the vehicle. The main advantage of such an indirect method is that the vehicle does not need to stop on the bridge, avoiding traffic disruption, and the same vehicle can be used to monitor a large stock of bridges.

Bridge natural frequencies have become one of the most commonly measured and monitored modal parameters in vibration-based SHM due to the relative ease with which they can be extracted for the purposes of damage detection [1, 8]. Frequencies are used as indicators of deterioration in structural condition, based on the principle that damage will cause a (global or local) change in the physical properties of the bridge, such as stiffness or mass, which in turn will cause a change in the dynamic properties, e.g. natural frequencies. As bridge frequencies of vibration are considered to remain constant in ideal conditions, any damage leads to changes in frequencies that should therefore be detectable.

However, bridge frequencies have been found to be sensitive to environmental influences, e.g. temperature and relative humidity, with relative frequency variations of up to and over 10% observed [9-12]. Several researchers have investigated these effects in practice [12-15] and highlight that operational loading conditions due to ongoing traffic also affect the frequency of the bridge, with an increase in mass generally causing a decrease in frequency. Methods for the filtering or removal of these environmental and operational influences have been proposed [11]. These include input-output methods, such as regression models [16, 17], and output-only methods, such as those derived from principal component analysis (PCA) and factor analysis [18, 19]. More recently, in [20] an improved independent component analysis method in frequency domain (ICA-F) was proposed and validated to extract dynamic properties for structures with either light or high damping.

For environmental influences such as temperature, variations follow diurnal and seasonal cycles. Reynders et al. [19] note that such changes therefore occur relatively slowly compared to a short monitoring time period that would correspond to a single vehicle bridge crossing event (e.g. 1.8 s to cross 40.4 m bridge span, travelling at 80 km/h). Hence, the bridge structure would be expected to behave in a linear time-invariant fashion with respect to temperature during this short time period. This indicates that environmental influences are of greater significance for longer-term bridge monitoring applications than for short-term, such as indirect bridge monitoring methods. On the other hand, the temperature influence can be cancelled performing investigations under laboratory conditions where temperature stays approximately constant.

However, the variation of bridge frequency during the passage of traffic across the bridge needs to be studied in greater detail, particularly for indirect monitoring methods, which rely on the response of the vehicle. Indirect methods currently focus on short to medium span bridges for which vehicle/bridge mass ratios are not insignificant and time-varying interaction between the vehicle and bridge needs to be considered. For example, Cantieni [21] reports observation of bridge frequency shifts of up to 0.7 Hz (23%). Most importantly, the author states that in order to explain these shifts, it is not sufficient to consider only the added mass of the vehicle; the coupling of bridge and vehicle needs to be considered. More recently, [22] reported frequency shifts up to 5.4% for a short span and relatively high (vehicle to bridge) mass ratio. Also, Kwon et al. [23] showed numerically that not only does the frequency of the bridge change while the vehicle passes, but the damping changes also. Moreover, even the shape of the mode shape varies with vehicle position, as reported in [24] based on an experimental campaign on an operational bridge.

In practice, the vehicle-bridge interaction (VBI) system will be time varying due to the movement of the vehicle along the bridge, evidenced by frequency variations identified in the literature. Traditionally the material and geometric properties of the vehicle and bridge would be assumed to remain unchanged during the interaction. However, with the bridge and vehicle coupled at their contact points, the entire system will change as the contact points of the vehicle move. This means that the instantaneous frequencies of the bridge will vary with time, i.e. with the passage of the vehicle across the bridge. This has implications for frequency monitoring

applications, both direct and indirect, as this range of variation needs to be accounted for, in addition to that resulting from other environmental sources.

Another level of complexity is that, not only is the response non-stationary, but also structural behaviour is non-linear. Clear non-linear relations between the vibration amplitude and the fundamental frequency of full-scale bridges have been reported [25, 26] and explained by the non-linear behaviour of the supports.

This paper aims at exploring further the variation of bridge frequencies during vehicle passage. In particular, the ultimate goal is to validate empirically that, not only is the added mass important, but also other mechanical properties of the traversing vehicle. This is achieved with a laboratory experiment using a scaled bridge and moving vehicle model. Under these conditions, there are no temperature variations that influence the results. The same vehicle is employed with two different suspension configurations. The beam response is investigated in two manners; directly, analysing the signals from accelerometers attached to the beam, and indirectly, examining the accelerations recorded on the vehicle. The signal processing is performed in the time-frequency domain using the continuous wavelet transform, in order to inspect the non-stationary and non-linear nature of the responses. The signal processing shows clear energy maps in time-frequency because of the use of one particular wavelet basis and combined with a convenient normalization strategy. Furthermore, interpretation of the results is aided with the support of a numerical model.

The paper is organized in the following way: Section 2 introduces the methods used, namely the experimental set-up, continuous wavelet transforms and the numerical model. Section 3 analyses the free-vibration responses of each of the subsystems separately, i.e. beam and vehicles. Section 4 examines the acceleration signals from the coupled response to quantify the frequency shift for each vehicle. This is done separately for direct measurements (sensor on the beam) and indirect measurements (sensors on the vehicles). The implications of these results on drive-by monitoring techniques are discussed in Section 5.

2. Methods

This section provides an overview of the experiments and tools used throughout this study. Section 2.1 describes the experimental set-up, giving details on the tested beam, traversing vehicle and instrumentation used. Section 2.2 briefly discusses time-frequency analysis of signals and introduces the continuous wavelet transform. Section 2.3 presents the numerical model used to evaluate the frequency evolution of the coupled vehicle and bridge system.

2.1. Experimental set-up

The experimental setup in the laboratory consisted of a scaled vehicle-bridge interaction model, shown in Figure 1. A two-axle vehicle model was moved across a simply supported beam at constant speed. Multiple vehicle crossings were measured for two different sets of suspension

properties for the vehicle. The responses of the beam and the traversing vehicle were recorded simultaneously.

(a)

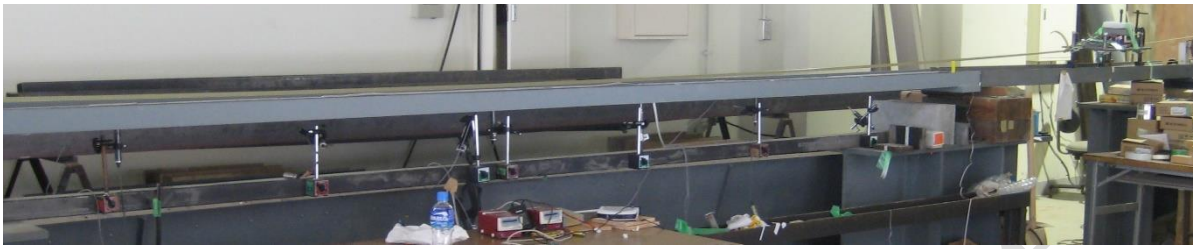

(b)

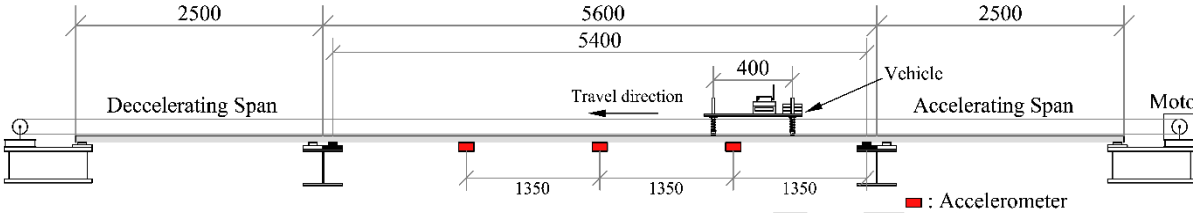

(c)

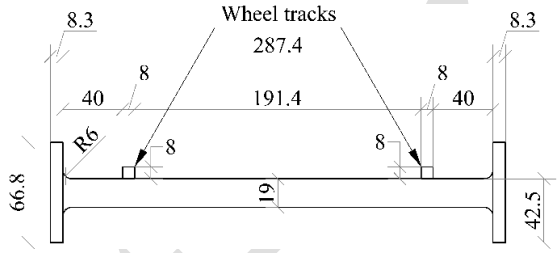

Figure 1: Experimental bridge and set-up; (a) Laboratory setup (b) Elevation of setup (c) Beam cross-section (units in mm).

2.1.1 Beam

A simply supported steel beam of span 5.4 m was adopted as the bridge model. This configuration was achieved using a pinned support at the beam entrance Figure 2(a) and with the roller (Figure 2(b)) located at the opposite end. All experimental bridge properties are given in Table 1. The first natural frequency of the beam was identified from free vibration tests as 2.69 Hz and this is discussed in greater detail in Section 3.1.

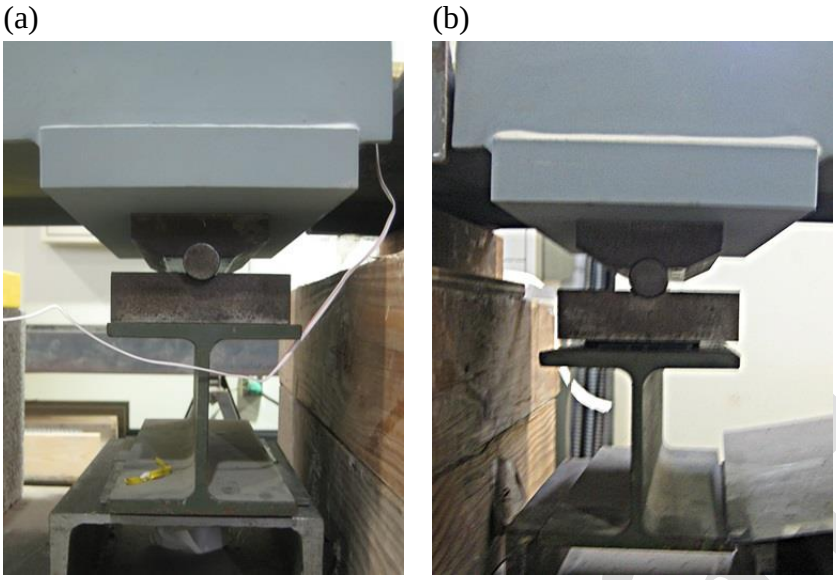

Figure 2: Beam support conditions (a) pinned support (b) roller support

Table 1 Beam properties

Property	Value	Unit
Span length, L	5.4	m
Modulus of elasticity, E	2.26×10^{11}	N/m^2
Second moment of area, I	5.77×10^{-7}	m^4
Material density, ρ	7800	kg/m^3
Cross sectional area, A	6.7×10^{-3}	m^2
Frequency of 1st bending mode, $f_{B,1}$	2.69	Hz

2.1.2 Vehicle

A two-axle model vehicle, shown in Figure 3, travelled across the beam at a constant speed, along the tracks shown in Figure 1(c), controlled by an electric motor and pulley system (Figure 4). A speed of 0.93 m/s was used in this investigation, equivalent to a full-scale vehicle speed of 20 km/h for an equivalent 40.4 m bridge. Scaling was based on a dimensionless speed parameter as outlined in [27]. The vehicle model had an adjustable configuration, enabling the variation of suspension properties during experiments; the axle stiffness could be adjusted by changing the suspension springs. The properties of the two vehicle configurations selected for this experimental programme are given in Table 2. The listed suspension properties correspond to updated stiffness values of the numerical models (Section 2.3) that best matched the measured free vibration frequencies of the vehicles (see Section 3.2). The axle spacing and track width for both models were 0.4 m and 0.2 m respectively.

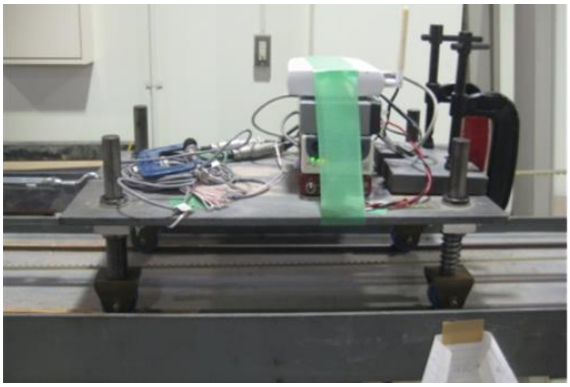

Figure 3: Experimental vehicle model

(a) (b)

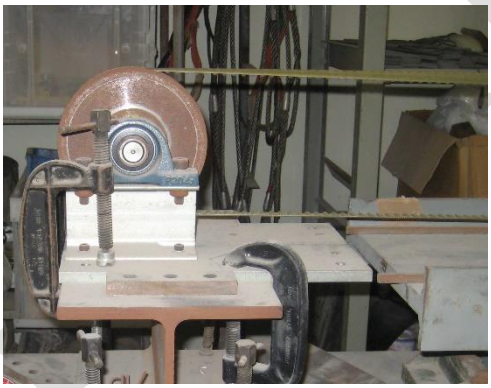

(c) (d)

Figure 4: Vehicle propulsion system (a) Electronic controller (b) pulley wheel (c) motor and pulley cable (d) cable hook/hitch on vehicle

It is important to note that the total mass (21.35 kg) and distribution to each axle is the same for each vehicle. Therefore, although the frequencies of vibration for vehicles V1 and V2 will differ due to the selected suspension spring stiffness, each model has the same mass ratio with the experimental bridge. Based on mass properties given in Table 1 and Table 2, the mass ratio can be calculated as 7.6%.

Table 2 Experimental vehicle properties

Property	Vehicle V1	Vehicle V2	Unit
Mass, m	21.35		kg
Moment of inertia, I_V	0.38		kg m^4
Wheelbase, d	0.4		m
Speed, v	0.93		m/s
Front suspension stiffness, k_1	2546.0	4075.5	N/m
Back suspension stiffness, k_2	4341.5	6944.5	N/m
First frequency, $f_{V,1}$	2.87	3.61	Hz
Second frequency, $f_{V,2}$	3.83	3.96	Hz

2.1.3 Instrumentation

The beam was instrumented with three Kyowa AS-1GB accelerometers (Figure 5(a)), with rated capacities of ±9.807 m/s^2 (±1 g). Two accelerometers of the same model were installed on the vehicle, one at the centre of each axle, to monitor its bounce and pitching motions, shown in Figure 5(b). A pair of strain gauges attached to hanging adhesive tape, as indicated in Figure 5(b), were utilised to identify vehicle entry and exit on the beam. Upon entry or exit of the vehicle, the tapes collided with a physical obstacle that produced distinct strain signals, which allowed the precise definition of entry and exit times. Two TML DC-104R dynamic strain recorder units, fitted with BA104 battery packs, were used for data acquisition and power supply; one stationary unit for the beam while the second unit was fitted to the vehicle. Vehicle measurements were monitored remotely during experiments via a wireless LAN connection; the recorder was connected to a SX-2500CG wireless Ethernet adapter by Silex Technology for this purpose (Figure 3). DC-7630 Dynamic Strain Recorder measurement software by TML was used for monitoring and collection of measured data during experimental testing. A sampling frequency of 100 Hz was used in all experiments.

(a) (b)

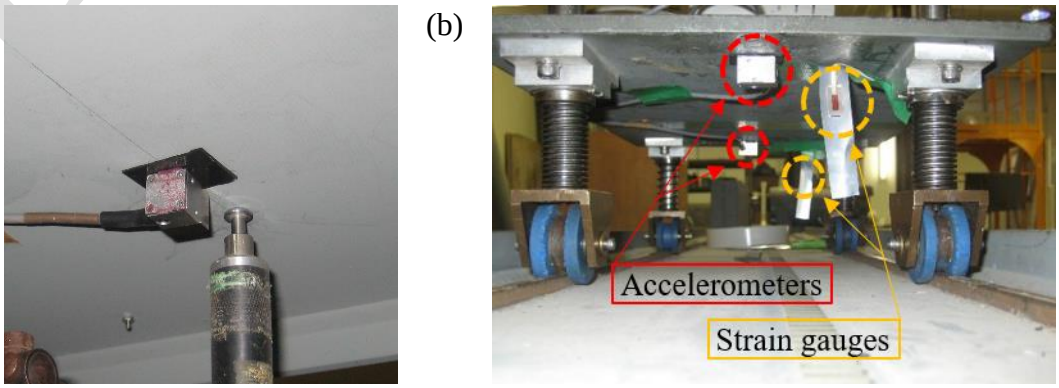

Figure 5: Sensors of experimental set-up: (a) accelerometer on beam (b) accelerometers and strain gauges on vehicle

2.2. Time-frequency analysis

It is common practice to analyse the responses of dynamical systems using the Fast Fourier Transform (FFT). However, this approach is inadequate when processing non-stationary and/or non-linear responses, characterized by significant variations in frequency content during short periods of time. The Continuous Wavelet Transform (CWT) is a better-suited tool, which offers a description of the frequency content in the time-frequency plane. It is a widely popular tool that was developed over three decades ago and many examples of its use can be found in the literature. For a comprehensive mathematical description of the CWT, the reader is referred to [28]. In summary, the CWT analysis results in a map of coefficients in the time-frequency plane derived from comparison of scaled and shifted versions of a basis function with the signal under investigation. There exists a wide variety of possible basis functions to be used and the final choice depends on the type of problem and the purpose of the analysis. The Modified Littlewood-Paley (MLP) basis is used in this study, which was first presented in [29]. This orthogonal wavelet basis was developed to optimize both the time and frequency localization properties simultaneously. Therefore, this study uses the CWT together with the MLP basis to analyse the measured accelerations from the laboratory experiment during free vibration (Section 3) and forced vibration (Section 4). This particular tool and basis is chosen because of its capacity for studying vehicle-bridge interaction problems, as shown for numerically generated responses in [30] and measured accelerations of a railway bridge during train passage in [31]. An inherent limitation of wavelet analysis is the so-called edge effect, which leads to unreliable results near the start and end of the signals. This problem can be corrected as suggested in [32] extending the signals using an autoregressive moving average model. However, in this study the analysed signals have been zero padded to move the influence of the edge effect sufficiently far away. This simple approach is deemed sufficient because all the measurements in this study have negligible energy at start and end of the signal. It is acknowledged that many other time-frequency tools are available (e.g. Short-Term Fourier Transform, Hilbert Huang, S-Transform) but these will not be discussed further here.

It is convenient to clarify two aspects of wavelet analysis relevant to the current research. First, the results from CWT are in terms of shift and scale parameters. While shift is directly proportional to time, there is no direct relationship between the scale parameter and frequency. Instead, it is possible to define a pseudo-frequency for each value of the scale parameter [31]. Strictly speaking, frequency and pseudo-frequency are not the same, but in practice these concepts are equivalent; hence only the term frequency is used throughout the remaining text. Second, the wavelet coefficients are normalized in terms of the instantaneous energy, which has been proven to be an effective strategy to improve the interpretation of energy maps [24]. This normalization removes the small variations due to varying levels of energy content in the signal and provides a clearer picture of how the energy content evolves in the time-frequency plane.

2.3. Numerical model

The experimental set-up is recreated numerically using a vehicle-bridge interaction model. The chosen numerical model is portrayed in Figure 6, a planar representation of a vehicle traversing a simply supported beam. The vehicle consists of a 2-DOF model with dissimilar suspension stiffness properties, as is the case for the experimental vehicle. The beam is described as an Euler-Bernoulli beam modelled using a finite element formulation. The equations of motion of both subsystems are defined separately in matrix form. As the vehicle moves along the beam, the systems of equations are coupled together accordingly, depending on the vehicle's position. Similar numerical models and solution procedures have been extensively used and reported in VBI literature. [27] provides a detailed description of the equations of motion and coupling procedure for precisely the same model. The particular numerical values of the model parameters are listed in Table 1 and Table 2.

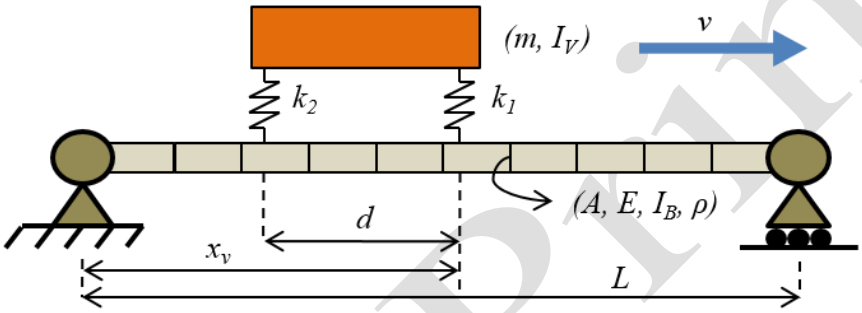

Figure 6: Sketch of vehicle-bridge interaction model

The numerical model is used in this study to estimate the system frequencies evolution during the vehicle's passage. In this sense, the model is used only to establish the coupled system of equations of motion for different vehicle positions. One eigenvalue analysis provides the "instantaneous" frequencies and, when repeated for each vehicle position, it is possible to retrieve the system frequencies and monitor their evolution. In order to simplify the interpretation of the results, damping is neglected in the present study and an un-damped modal analysis is performed. This assumption is reasonable since the particular damping ratios of the bridge and vehicles have been shown to be small [27].

3. Free vibration

In this section, analysis of free vibration tests carried out independently on the experimental bridge and vehicle models is presented. The purpose of this testing was to identify the properties of each independent dynamic system prior to analysing the effect of vehicle-bridge interaction on the dynamics of the coupled system. Furthermore, this testing enabled analysis of the results in the time-frequency domain, providing some important observations, which have implications for vehicle-bridge interaction/forced vibration presented in Section 4.

3.1. Beam

The free vibration response at mid-span of the experimental bridge is shown in Figure 7(a). As the focus of this experimental investigation was the evolution of frequency during dynamic

vehicle-bridge interactions, initially the bridge acceleration free vibration signals such as this, were studied in the time-frequency domain, as shown in Figure 7(b). This is carried out by processing the accelerations using the Continuous Wavelet Transform (CWT) with the Modified Littlewood-Paley (MLP) basis, and normalising the resultant wavelet coefficients by the instantaneous energy for each point in time. This normalisation is important as it delivers a better visualisation of the evolution of the frequency content. Note that in Figure 7(b) and similar figures, the colour white indicates areas equivalent to zero, or low, energy levels while dark red indicates areas equivalent to high energy levels.

The acceleration signals have been zero padded by a length of 2 seconds at each end. Figure 7(b) shows grey shaded areas that indicate the regions, or cone of influence, where the results are not so reliable due to the edge effects associated with the CWT. Note that the high values observed in the CWT before 5 s and after 20 s have no physical meaning. They are simply artefacts due to the normalization and small magnitude of the signals at those times. Studying the free vibration in the time-frequency domain, comparing Figure 7(a) and Figure 7(b), it can be seen that the frequency changes slightly during free vibration, depending on the vibration magnitude i.e. the frequency increases as the vibration amplitude decreases. This clearly shows that the beam response on its own is non-linear. The reasons for this might be material non-linearity, with a larger influence from support non-linear behaviour. Similar non-linear responses have been reported on full-scale bridges before, for instance in [25] and [26].

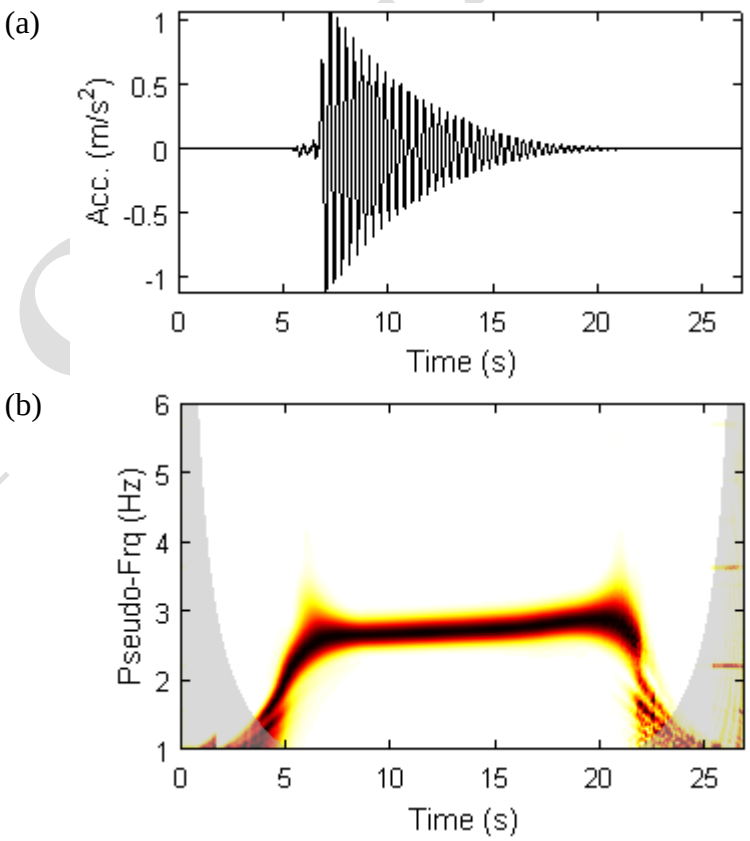

Figure 7: Beam free vibration; (a) acceleration signal; (b) normalised CWT analysis (shaded areas = edge effects, cone of influence)

The same bridge acceleration signal can also be studied in the frequency domain only. The acceleration signal is processed using the Fast Fourier transform (FFT) to give the Power Spectral Density, which is plotted in Figure 8(a) and indicates that the beam's fundamental frequency in free vibration is 2.69 Hz (indicated by dashed blue lines in Figure 8). However, as can be seen in the time-frequency decomposition in Figure 7(b), the frequency does not remain strictly constant during free vibration. Thus, studying the signal in the frequency domain only as per Figure 8(a) would not provide an accurate representation of the bridge behaviour. Therefore, to further investigate the relationship between the amplitude of vibration and fundamental frequency, the acceleration signal is analysed with the Hilbert transform; a description and example of usage of the Hilbert transform can be found in [25].

The original signal is band-pass filtered around 2.69 Hz with a total band width of 4 Hz. Then, the Hilbert transform is performed. The magnitude of the Hilbert transform provides an estimate of the instantaneous amplitude of the signal. Figure 8(b) shows the obtained instantaneous amplitude, to which an exponential curve is fitted (red curve in Figure 8(b)) to smooth out the result. It is also possible to obtain the instantaneous frequency from the Hilbert transform. This is shown in Figure 8(c) and a quadratic curve is fitted to the results. Finally, the non-linear relationship between frequency and amplitude is given in Figure 8(d) based on the fitted results. As a reference, the extracted frequency from the PSD in Figure 8(a) is also shown as a blue dashed line. The mass of the system does not change in free vibration, which indicates that the stiffness of the beam system increases as the vibration amplitude decreases. This increase is caused by friction at the support (boundary) conditions and is not insignificant - the frequency range of 2.65 Hz to 2.8 Hz represents a change in frequency of up to 5.7%. These variations in frequency due to non-linear effects need to be accounted for when studying the forced vibration in Section 4.

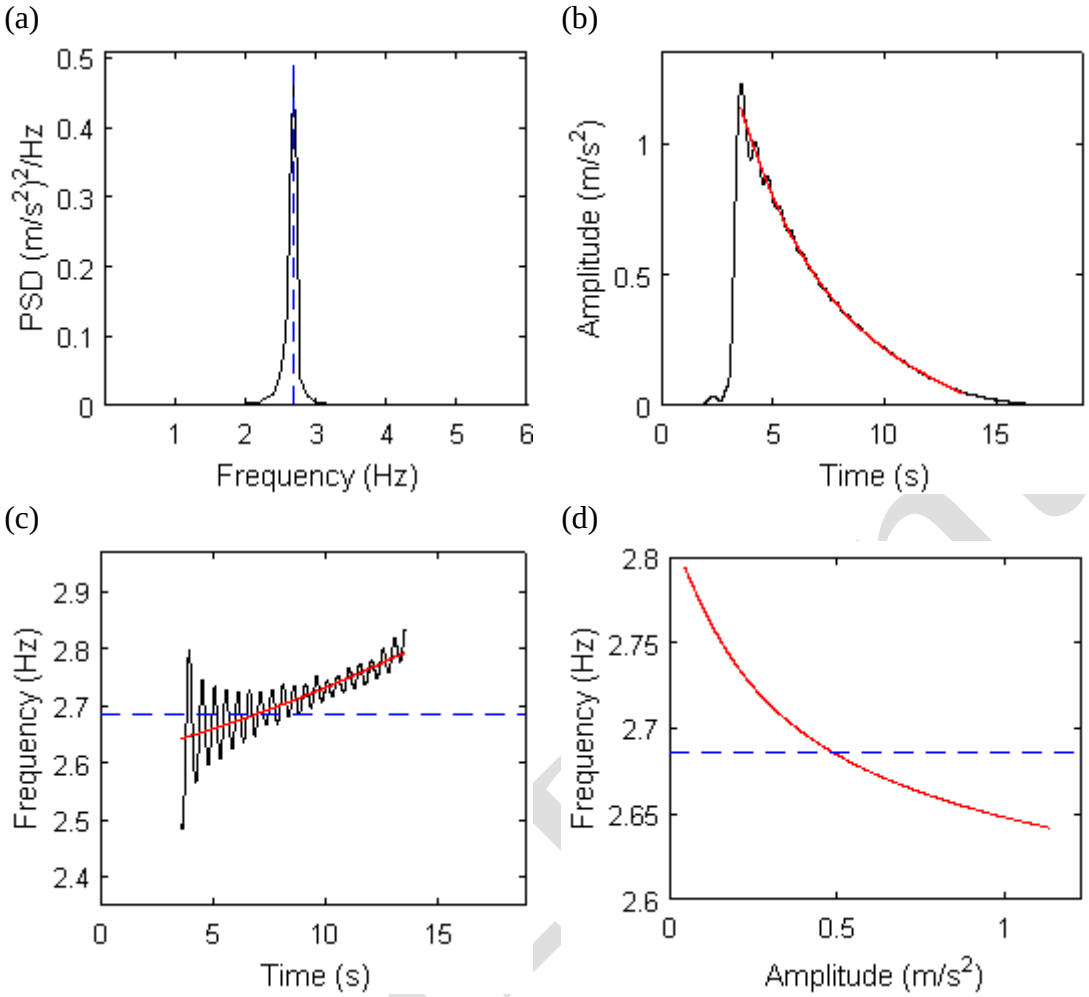

Figure 8: Beam free vibration; (a) PSD; (b) instantaneous amplitude; (c) instantaneous frequency; (d) non-linear frequency to amplitude relation (dashed blue line = extracted frequency; solid black line = Hilbert transform results; solid red line = fitted curves)

3.2. Vehicles

Following the analysis of the bridge free vibration response, it is beneficial and convenient to study the acceleration response in free vibration of the experimental vehicle models in the time-frequency domain, enabling a clear identification of the vehicles system's frequencies. Similar to the bridge accelerations, the vehicle's acceleration signals have been zero padded by a length of 4 seconds at each end. For the free vibration of the experimental vehicle model V1 (see Figure 9(a)), if only the acceleration spectrum of the signal is obtained, as shown in Figure 9(b), then only one single frequency can be extracted, which is 2.88 Hz. However, it is expected that the experimental model response should exhibit two main frequencies corresponding to bounce and pitch motions. These two separate frequencies can be clearly identified if the free vibration response is studied in the time-frequency domain as shown in Figure 9(c). Extracting the vehicle system's frequencies based on this figure gives values of 2.87 Hz and 3.83 Hz, corresponding to bounce and pitch respectively. During the early part of the free vibration (up to 8 s), the first mode (2.87 Hz) dominated the response; this is reflected in Figure 9(c). Following this period, most of the energy of the signal was dissipated by the inherent

suspension damping. However, the vehicle continued to vibrate with low amplitude until around 12 s, with its response dominated by its second mode (3.83 Hz). Due to the low vibration amplitude, this frequency does not appear in Figure 9(b). However, due to the normalisation by the instantaneous energy it is possible to see both frequencies clearly in Figure 9(c).

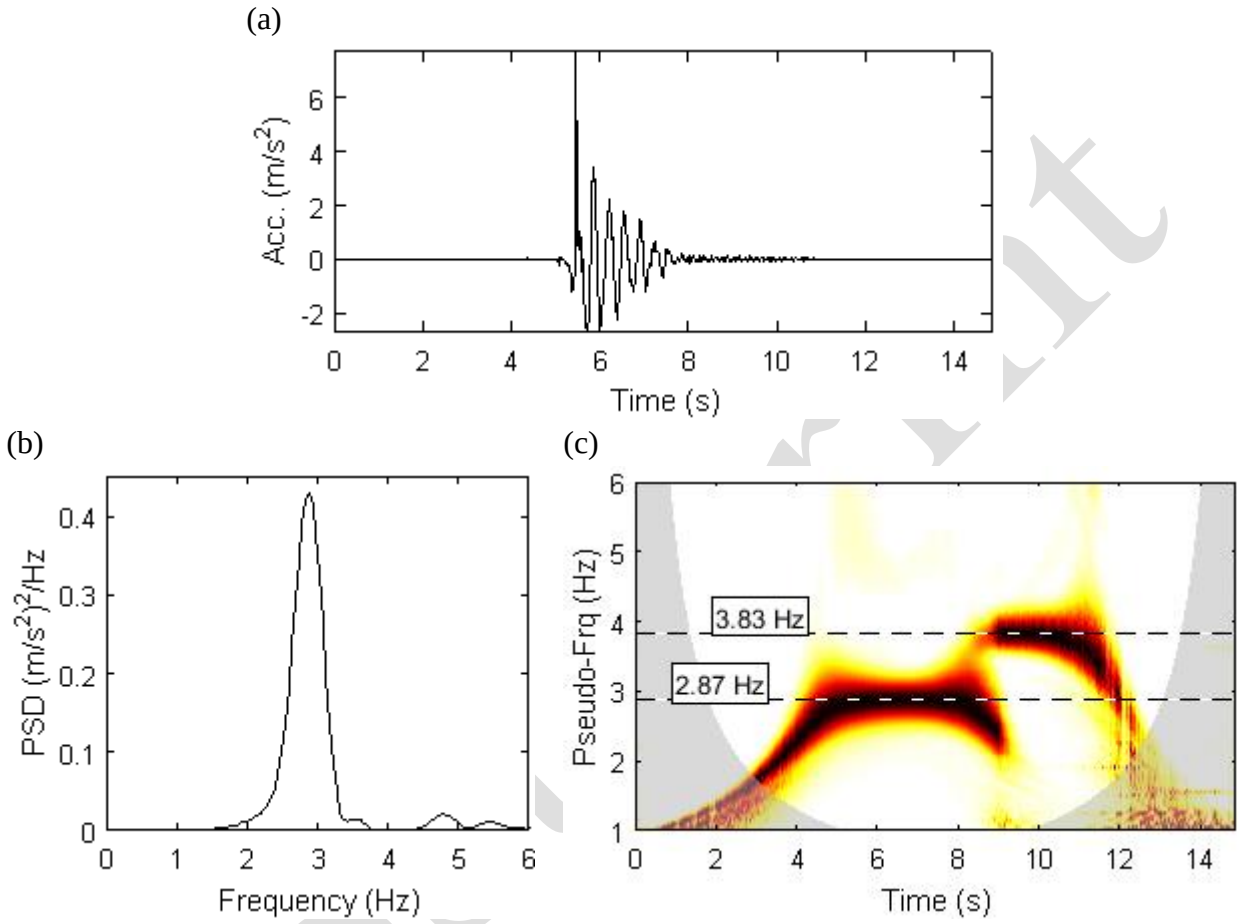

Figure 9: Vehicle V1 free vibration: (a) acceleration signal; (b) PSD; (c) normalised CWT analysis (dashed lines = extracted frequencies; shaded areas = edge effects, cone of influence)

The processed free vibration acceleration responses of vehicle model V2 are shown in Figure 10. Unlike the spectra obtained for vehicle V1 (Figure 9(b)), here it is possible to estimate the vehicle frequencies as 3.61 Hz and 3.96 Hz directly from the peaks in the free vibration acceleration spectra signal (Figure 10(a)). Therefore, for this particular vehicle model, it is not strictly necessary to show the results in the time-frequency domain. However, the wavelet analysis still produces some interesting results, shown in Figure 10(b). Comparing this figure with Figure 9(b), it can be observed that two clear distinct bands, one for each vehicle frequency, do not appear. Instead, the cancelling points of the beat wave resulting from closely spaced frequencies can be appreciated. The duration between these cancellation points is approximately 2.9 s, which corresponds to the inverse of the difference between frequencies, namely 0.35 Hz.

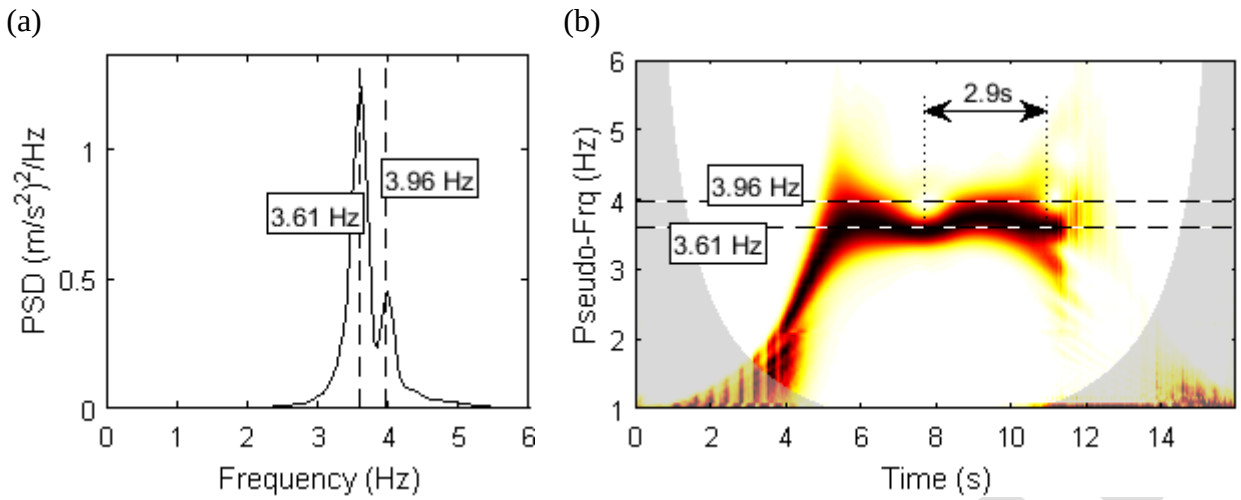

Figure 10: Vehicle V2 free vibration: (a) PSD; (b) normalised CWT analysis (dashed lines = extracted frequencies; shaded areas = edge effects, cone of influence)

The extracted free vibration frequencies of V1 and V2 were used to perform model updating of the vehicle numerical models. In particular, the suspension properties (listed in Table 2) were updated to match their corresponding free vibration frequencies.

4. Forced vibration

The dynamic responses of both the vehicle and the bridge during the vehicle crossing, i.e. under forced vibration, are quite different to those observed under free vibration and are analysed in this section. As the vehicle crosses over the bridge, there is a dynamic interaction between them, i.e. their dynamic responses are coupled via the wheel contact points. This results in a time-varying vehicle-bridge dynamic interaction system, as opposed to the independent dynamic sub-systems analysed for free vibration in Section 3. It follows that the modal properties of the overall system will vary as the vehicle changes position as it crosses the bridge. The observed frequencies of both subsystems (vehicle and beam) will undergo corresponding changes. In order to analyse these changes, similar to Section 3, vehicle and bridge acceleration responses under forced vibration due to a vehicle crossing are processed here using the fast Fourier transform (FFT) and further analysed in the time-frequency domain via CWT.

4.1. Beam

Examples of the processed spectra for the vehicle-induced bridge mid-span acceleration response are shown in Figure 11. Figures 11(a) and (b) correspond to one crossing of vehicle V1, while Figures 11 (c) and (d) correspond to one crossing of vehicle V2. For each vehicle, the bridge acceleration spectra show a series of peaks that do not correspond to the frequencies of the Beam (B) and vehicles (V) extracted during free vibration (shown as dashed vertical lines).

Studying these signals in the time-frequency domain, the CWT responses illustrate the evolving energy content. The calculated frequency evolutions obtained from the numerical model outlined in Section 2.3 are superimposed here using dashed lines. There is no perfect match between the experimental measurements and the instantaneous frequencies predicted by the numerical model, but the trend of both with time is similar. In particular, the fundamental frequency of the bridge clearly changes during forced vibration, and that change follows the same trend as predicted by the numerical model, with the largest deviation occurring between 5 and 6 seconds when the vehicle is passing over the bridge's mid-span. It is also of note in the experimental response that during free vibration, following the vehicle exit from the bridge, the bridge vibration follows the increasing trend observed earlier in Figure 7(b).

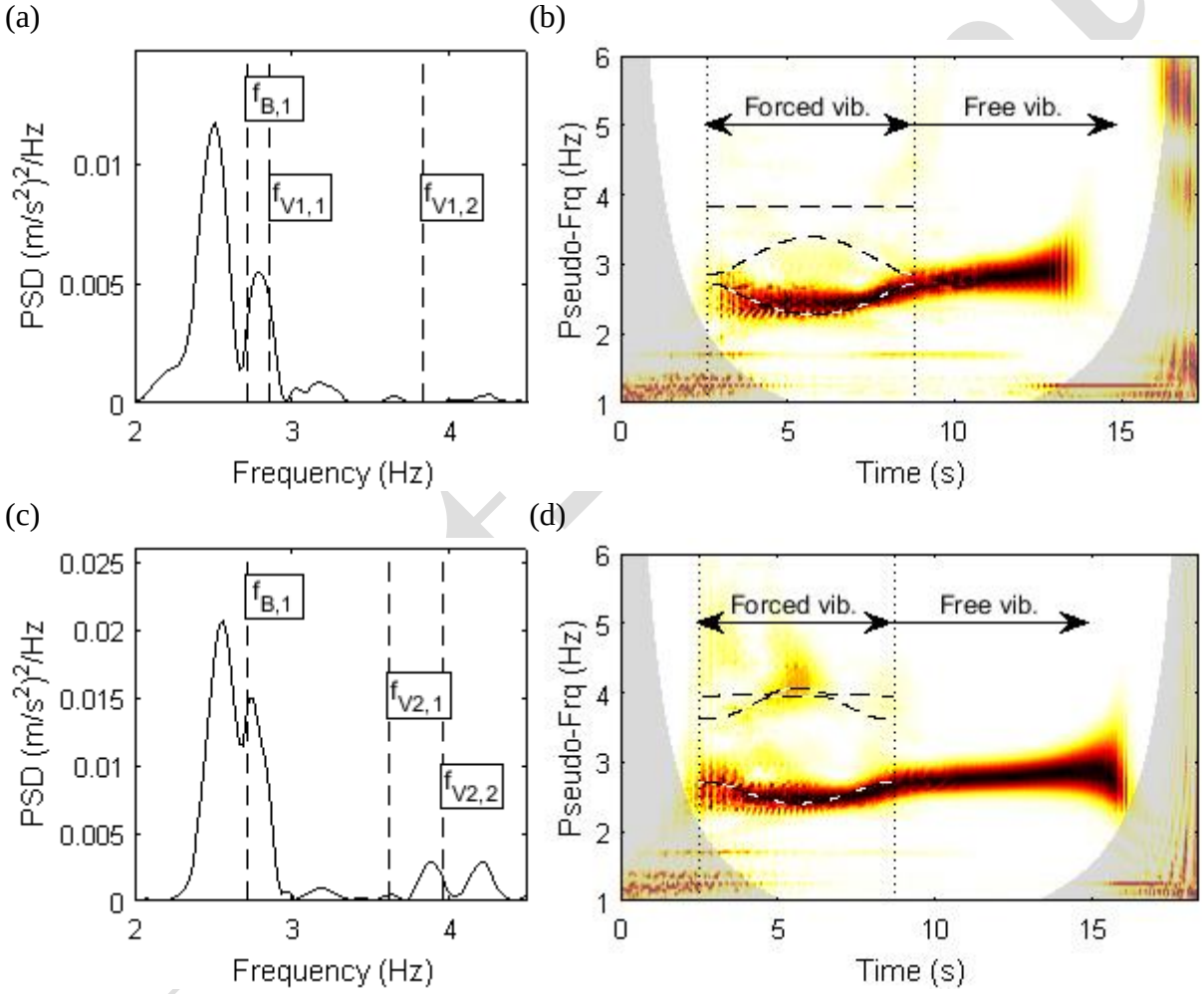

Figure 11: Beam mid-span response in forced vibration; (a) PSD for V1; (b) normalised CWT for V1; (c) PSD for V2 (d) normalised CWT for V2.

In the laboratory experiment, each vehicle crossing was repeated five times, providing five bridge measurement sets for each vehicle model. The acceleration signals of the beam at mid-span have been analysed in the time-frequency domain via the normalized CWT and are presented in Figure 12. The CWT was performed exclusively in a frequency range (2 to 3 Hz) near the bridge fundamental frequency while the number of evaluated scales was increased to provide a clearer frequency resolution. The CWT coefficients are shown here for the time

instant when the centre of gravity of the vehicle is at mid-span, which corresponds to the situation where maximum frequency shifts can be expected. This figure also shows the smoothed average CWT coefficients for each vehicle. The dashed vertical line in Figure 12 corresponds to the reference fundamental frequency of the beam extracted in free vibration (see Figure 8(a)), while the shaded area corresponds to the expected possible range of values of the fundamental frequency according to the amplitude-frequency relation obtained in Figure 8(c).

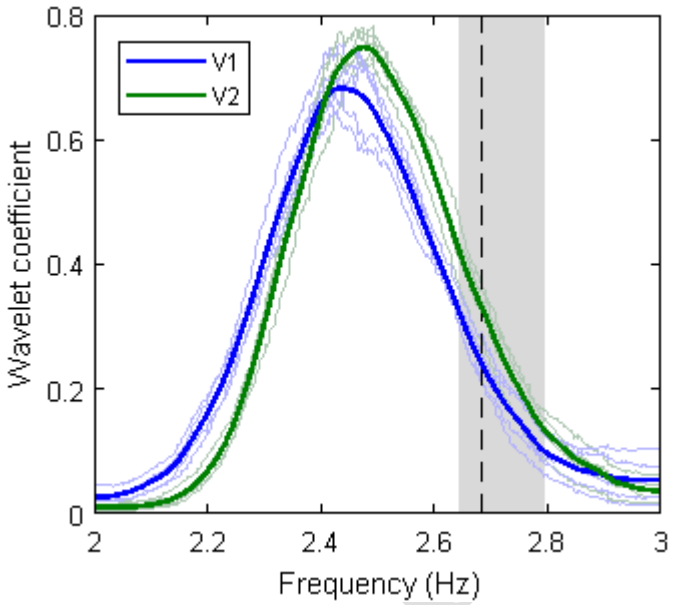

Figure 12: CWT coefficients at the moment of maximum frequency shift (thin solid lines = individual crossing; thick solid lines = smoothed average result for each vehicle; dashed line = beam's fundamental frequency in free vibration; shaded area = variability due to non-linearities)

Therefore, Figure 12 can be used for the purposes of analysing the maximum deviations from the reference bridge fundamental frequency. It can be seen from this figure that each vehicle produces a different frequency shift despite their masses being the same. The average results indicate that the bridge's frequency is 2.43 Hz for V1 and 2.48 Hz for V2 at the time instants when the vehicles are crossing the mid-span. The vehicle V1 produces the larger frequency shift (a decrease of 9.69 %) compared to vehicle V2 (a decrease of 7.84 %). This can be attributed to the frequency ratio, defined as the ratio of the lowest vehicle frequency to the bridge's fundamental frequency in free vibration. As shown in a previous numerical study [30] for a 1-DOF vehicle crossing a beam, larger shifts in the bridge frequency are expected for frequency ratios closer to one. In other words, when there is a closer match between bridge and vehicle frequencies, there exist larger frequency shifts due to the coupling of the two subsystems.

In order to assess the influence of the frequency ratio for the particular configuration of this experiment, the results from the numerical model and the experimental results are compared in Figure 13. Firstly, the figure shows the beam's fundamental frequency in free vibration as obtained in Section 3.1. This is the reference frequency and the target for the drive-by system

analysing the vehicles' accelerations. However, due to the coupling effects between bridge and vehicle the process is non-stationary and leads to varying frequencies for every new vehicle position. The maximum frequency shifts were obtained experimentally for each vehicle and plotted in Figure 13 in terms of each vehicle's frequency ratio. Additionally, the maximum frequency shift is calculated numerically using the model presented in Section 2.3. The suspension properties of the vehicle are scaled within a range of values, while keeping the ratio between front and back suspension stiffness constant. By doing so, the resulting numerical models included the two particular models that described vehicles V1 and V2.

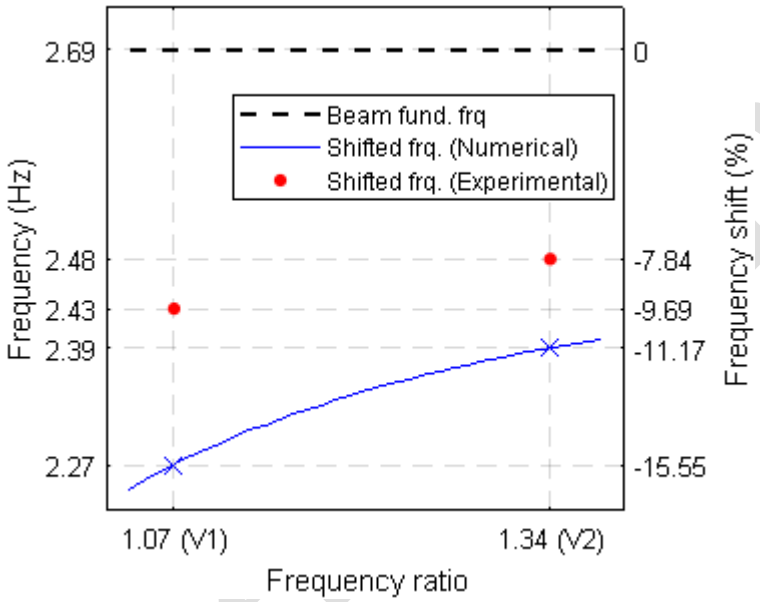

Figure 13: Comparison of experimental and numerical results

The direct comparison of experimental and numerical results in Figure 13 shows poor agreement but a similar trend. The disagreement between results can be attributed to the relative simplicity of the numerical model and to minor discrepancies with the numerical properties used for modelling the physical beam and vehicles. For these reasons, the numerical results should be regarded only as indicative on how the frequencies might change with frequency ratio.

4.2. Vehicle

Figures 14(a) and (b) show the CWTs of vehicle V1 and V2 accelerations respectively, recorded over axle 2 for one bridge crossing each. These responses correspond to Figures 11(b) and (d) respectively for the numerical model. The results show that during forced vibration, these acceleration signals contain some information about the bridge's frequency, with a clearer match observed between the numerical model and experiment for vehicle V1. In addition, it could be argued that some frequency shift is observed for the vehicle frequencies. However, the results in general are not so clear, with occurrence of some frequencies in the CWT response that were not observed in earlier tests. These can be attributed to the effects of the surface profile, the propulsion system on the vehicle and other sources of noise. After the vehicle has

left the bridge, the propulsion system is shut off and the vehicle abruptly comes to rest. The corresponding time histories after 12 s in the CWTs for each vehicle show clear bands indicating the free vibration frequencies of the vehicles, observed earlier in Figure 9 and Figure 10.

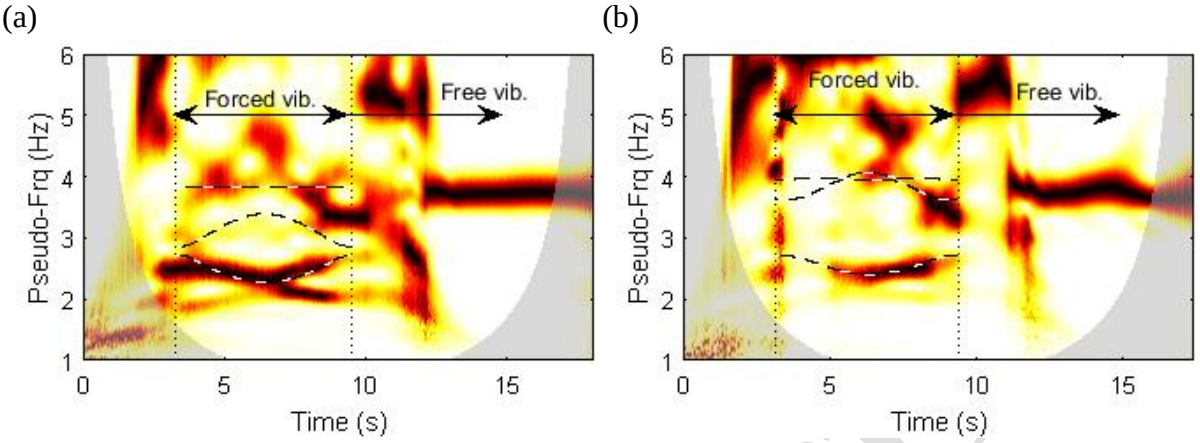

Figure 14: CWT of vehicle acceleration; (a) V1; (b) V2

5. Discussion

The frequency evolutions in time and frequency observed in the results presented in this paper highlight important aspects that should be considered in the field of vehicle-bridge interaction (VBI) dynamics. It is most relevant for vibration-based bridge monitoring approaches that rely on vehicle excitation. Although there is an awareness of the time-varying nature of VBI, this is generally attributed to the contribution of the added mass of the vehicle on the bridge. However, this study has shown that vehicles of the exact same mass passing over the same bridge at the same speed but with different suspension properties will cause different frequency shifts of the bridge's fundamental frequency. Hence, frequency shifts depend, not only on the mass, but also on other mechanical properties of the vehicle. In this study, the magnitudes of these shifts are also greater than those frequency shifts expected due to the driving frequency ($\pm v/2L$ in Hz) [5]. Therefore, any indicator of structural performance based on dynamic properties needs to be more sensitive to the bridge condition than to the variation in system dynamics highlighted by these frequency shifts. Furthermore, different vehicles or variation in the total number of vehicles on a bridge will change the frequency shift, with the measured bridge frequency falling within a potential range of shifted frequencies around the bridge's fundamental frequency. However, if this range can be identified for a particular bridge, it may be possible to overcome the effect of the shift. Further work is required in this regard.

This also highlights a significant challenge for indirect (or drive-by) bridge monitoring approaches that aim to identify the bridge frequency or bridge dynamic parameters from the vehicle's acceleration responses. Similarly, different instrumented vehicles will cause different frequency shifts, even before considering the effect of additional traffic (i.e. more than one vehicle) on the bridge. If a priori information about the bridge or free vibration measurements are unavailable (before the initial pass over the bridge), a drive-by monitoring system would have difficulty in extracting bridge parameters without some additional form of excitation. The

authors believe that the cost of additional excitation, or the time-related cost required in obtaining information about the bridge dynamic response, starts to become prohibitive for drive-by approaches relative to periodic visual inspections and thus the benefit of a fast, preliminary bridge condition screening may be lost. However, a drive-by system using a single calibrated vehicle could potentially be used to monitor changes in a coupled VBI dynamic response. This is done for instance in [33, 34] by monitoring the vehicle response before, during and after a bridge crossing. Another promising solution is the development of the analytical formula, as suggested in [35], for a vehicle passing over the bridge in order to remove the effects of the frequency variation caused by VBI.

The results presented here confirm the effect of the vehicle suspension properties on the bridge frequency. However, the direct applicability of the results is limited because of the site-specific nature of the problem and the chosen scaling of the experimental models. For these reasons, the numerical values cannot be simply extrapolated to any vehicle-bridge system. Nevertheless, the findings are still valid and relevant. The effect of suspension properties is case specific, but strongly correlated to the mass and frequency ratios between vehicle and bridge. The experimental results ratify that larger frequency shifts can be expected for frequency ratios closer to one, as the theoretical and numerical analysis had indicated. On the other hand, the particular results presented here are based on scaled models. The scaled beam represents a 40.4 m long steel bridge described in [36], with a total bridge mass of 305 tonnes and fundamental frequency of 2.33 Hz. With this information, it is possible to obtain the properties of an equivalent full-scale vehicle maintaining the mass and frequency ratios of the scaled experiment. The equivalent full-scale vehicle would correspond to a 23 tonnes 2-axle vehicle with frequencies 2.49 and 3.32 Hz. This vehicle might be unrealistic in terms of gross vehicle weight but not far from a plausible worst-case scenario vehicle.

Finally, future investigations should further explore the non-linearity of bridge vibrations. It might be desirable to widen the extent of amplitudes in which the non-linear relation is defined. In other words, to increase the maximum amplitude of the accelerations of the beam in free vibration, obtaining a broader definition range of the bridge non-linearity.

6. Conclusion

This paper investigated, in a laboratory experiment, the evolution of bridge frequencies during the passage of a vehicle. The results validate and quantify the effect of the vehicle to bridge frequency ratio on the shift of the fundamental frequency of the beam. This was achieved by investigating the responses for two different vehicle stiffness configurations while maintaining the same mass ratio. The results confirm that it is not only the added mass that is important in the coupling of vehicle-bridge systems, but also the mechanical properties of the traversing vehicles. The experimental results show that the vehicle with a frequency ratio closer to unity produces larger shifts of the bridge's frequency. This conclusion is in line with the predictions and trends observed in numerical simulations.

Furthermore, it has been argued and shown that the responses are not only non-stationary, but also non-linear. It has been demonstrated that such a response must be analysed in the time-frequency domain. Here, the processing of the measured signals provided clear representations of evolution of the energy content that resembled the numerical predictions. This was accomplished using the continuous wavelet transform with the Modified Littlewood-Paley basis, together with a normalization strategy in terms of the instantaneous energy.

Moreover, the experimental responses were investigated in free-vibration (uncoupled system) and forced-vibration (coupled system), as well as directly (beam responses) and indirectly (vehicle responses). It was shown that time-frequency signal processing of the signals in free vibrations aids extraction of the system frequencies and offers valuable information about possible non-linearities. On the other hand, the analysis of the direct measurements offered much clearer frequency evolution descriptions compared to the indirect measurements. This highlights the difficulties faced by any technique that aims at extracting the bridge frequency from a passing vehicle.

The results are particularly relevant for indirect or drive-by monitoring techniques. Further investigations are required in order to understand how the frequencies change and to propose correction strategies on the inferred modal properties extracted by traversing vehicles.

Acknowledgements

The authors wish to express their gratitude and appreciation to Prof. M. Kawatani and Mr. T. Toshinami for their support and assistance during the experimental programme.

The experimental programme was undertaken with the support of the Japanese Society for the Promotion of Science Postdoctoral Fellowship for North American and European Researchers (Short Term), and the 7th European Framework ASSET (Advanced Safety and Driver Support in Efficient Road Transport) project.

References

[1] Carden EP, Fanning P. Vibration based condition monitoring: A review. *Structural Health Monitoring*, 2004; 3: 355–377.
[2] Chang PC, Flatau A, Liu SC. Review Paper: Health Monitoring of Civil Infrastructure. *Structural Health Monitoring*, 2003; 2: 257–267.
[3] Farrar C, Worden K. An introduction to structural health monitoring. *Philosophical Transactions of the Royal Society A*, 2007; 365: 303–315.
[4] Brownjohn JMW. Structural health monitoring of civil infrastructure. *Philosophical Transactions of the Royal Society A*, 2007; 365: 589–622.
[5] Yang YB, Lin CW, Yau, JD. Extracting bridge frequencies from the dynamic response of a passing vehicle. *Journal of Sound and Vibration*, 2004; 272: 471–493.

[6] Malekjafarian A, McGetrick PJ, OBrien EJ. A review of indirect bridge monitoring using passing vehicles. *Shock and Vibration*, 2015; Article ID: 286139.
DOI: 10.1155/2015/286139.
[7] Kim CW, Kawatani M. Challenge for a Drive-by Bridge Inspection. In: *Proceedings of the 10th International Conference on Structural Safety and Reliability (ICOSSAR2009)*, Osaka, Japan, 13-17 September 2009, pp. 758-765.
[8] Salawu OS. Detection of structural damage through changes in frequency: A review. *Engineering Structures*, 1997; 19: 718–723.
[9] Peeters B, De Roeck G. One-year monitoring of the Z 24-Bridge: environmental effects versus damage events. *Earthquake Engineering Structural. Dynamics*, 2001; 30: 149–171.
[10] Sohn H. Effects of environmental and operational variability on structural health monitoring. *Philosophical Transactions of the Royal Society A*, 2007; 365: 539–60.
[11] Cunha Á, Caetano E, Magalhães F, Moutinho C. Recent perspectives in dynamic testing and monitoring of bridges. *Structural Control and Health Monitoring*, 2013; 20, 853–877.
[12] Brownjohn JMW, Westgate R, Koo K, Cross EJ. Identifying and discriminating thermal effects for structural health monitoring. In*: Proceedings of the Second Conference on Smart Monitoring, Assessment and Rehabilitation of Civil Structures (SMAR 2013)*, 9th –11th September 2013, Istanbul, Turkey.
[13] Cross EJ, Worden K, Koo KY, Brownjohn JMW. Filtering environmental load effects to enhance novelty detection on cable-supported bridge performance. In: *Proceedings of the Sixth International Conference on Bridge Maintenance, Safety and Management (IABMAS)*, 2012; pp. 745–752.
[14] Cross EJ, Koo KY, Brownjohn JMW, Worden K. Long-term monitoring and data analysis of the Tamar Bridge. *Mechanical Systems and Signal Processing*, 2013; 35: 16–34.
[15] Koo KY, Brownjohn JMW, List DI, Cole R.. Structural health monitoring of the Tamar suspension bridge. *Structural Control and Health Monitoring*, 2013; 20: 609–625.
[16] Hair J, Anderson R, Tatham R, Black W. *Multivariate Data Analysis*. Prentice Hall: New Jersey, 1998.
[17] Yang DH, Yi TH, Li HN, Zhang YF. Correlation-based estimation method for cable-stayed bridge girder deflection variability under thermal action. *ASCE Journal of Performance of Constructed Facilities*, 2018, 32: 1-10.
[18] Deraemaeker A, Reynders E, De Roeck G, Kullaa J. Vibration-based structural health monitoring using output-only measurements under changing environment. *Mechanical Systems and Signal Processing*, 2008; 22: 34–56.
[19] Reynders E, Wursten G and De Roeck G. Output-only structural health monitoring in changing environmental conditions by means of nonlinear system identification. *Structural Health Monitoring*, 2013; 13: 82–93.
[20] Yao XJ, Yi TH, Qu C. Blind modal identification in frequency domain using independent component analysis for high damping structures with classical damping. *Computer-Aided Civil and Infrastructure Engineering*, 2018, 33: 35-50.
[21] Cantieni R. *Investigation of vehicle-bridge interaction for highway bridges. Heavy vehicles and roads: technology, safety and policy*. Thomas Telford, London, 1992.

[22] Kim CY, Jung DS, Kim NS, Kwon SD, Feng MQ. Effect of vehicle weight on natural frequencies of bridges measured from traffic-induced vibration. *Earthquake Engineering and Engineering Vibration*, 2003; 2: 109-115.
[23] Kwon SD, Kim CY, Chang SP. Change of modal parameters of bridge due to vehicle pass. In: *23rd Conference and Exposition on structural dynamics (IMAC-XXIII)*, 2005.
[24] Cantero D, Hester D, Brownjohn J. Evolution of bridge frequencies and modes of vibration during truck passage. *Engineering Structures*, 2017; 152: 452-464.
[25] Gonzalez I, Karoumi R. Analysis of the annual variations in the dynamic behavior of a ballasted railway bridge using Hilbert transform. *Engineering Structures*, 2014; 60: 126–132.
[26] Ülker-Kaustell M, Karoumi R. Influence of rate-independent hysteresis on the dynamic response of a railway bridge. *International Journal of Rail Transportation*, 2013; 1: 237-257.
[27] McGetrick PJ, Kim CW, González A, OBrien EJ. Experimental validation of a drive-by monitoring system for bridges. *Structural Health Monitoring*, 2015; 14: 317–331.
[28] Cohen A, Ryan RD. *Wavelets and Multiscale Signal Processing*. Chapman & Hall, Boundary Row, London, 1995.
[29] Basu B, Gupta VK. Seismic response of SDOF systems by wavelet modeling of nonstationary processes. *Journal of Engineering Mechanics*, 1998; 124: 1142-1150.
[30] Cantero D, OBrien EJ. The Non-Stationarity of Apparent Bridge Natural Frequencies During Vehicle Crossing Events. *FME Transactions*, 2013; 41: 279-284.
[31] Cantero D, Ülker-Kaustell M, Karoumi R. Time–frequency analysis of railway bridge response in forced vibration. *Mechanical Systems and Signal Processing*, 2016; 76: 518–530.
[32] Li H, Yi T, Gu M, Huo L. Evaluation of earthquake-induced structural damages by wavelet transform. *Progress in Natural Science*, 2009; 19: 461-470.
[33] McGetrick PJ, Hester D, Taylor SE. Implementation of a drive-by monitoring system for transport infrastructure utilising smartphone technology and GNSS. *Journal Civil Structural Health Monitoring*, 2017; 7: 175-189.
[34] González A, Covián E, Madera J. Determination of Bridge Natural Frequencies Using a Moving Vehicle Instrumented with Accelerometers and GPS. In: *Proceedings of the Ninth International Conference on Computational Structures Technology*, Athens, Greece, paper 281, 2008.
[35] Chang KC, Kim CW and Borjigin S. Variability in bridge frequency induced by a parked vehicle. *Smart Structures and Systems*, 2014; 13: 755-773.
[36] Kim CW, Kawatani M, Kim KB. Three-dimensional dynamic analysis for bridge-vehicle interaction with roadway roughness. *Computers and Structures*, 2005; 83: 1627-1645.